In vivo reprogramming of Sox9$^+$ cells in the liver to insulin-secreting ducts

Anannya Banga, Ersin Akinci, Lucas V. Greder, James R. Dutton, and Jonathan M. W. Slack[1]

Stem Cell Institute, McGuire Translational Research Facility, University of Minnesota, Minneapolis, MN 55455

Edited by Kenneth S. Zaret, University of Pennsylvania School of Medicine, Philadelphia, PA, and accepted by the Editorial Board August 3, 2012 (received for review January 30, 2012)

In embryonic development, the pancreas and liver share developmental history up to the stage of bud formation. Therefore, we postulated that direct reprogramming of liver to pancreatic cells can occur when suitable transcription factors are overexpressed. Using a polycistronic vector we misexpress *Pdx1*, *Ngn3*, and *MafA* in the livers of NOD-SCID mice rendered diabetic by treatment with streptozotocin (STZ). The diabetes is relieved long term. Many ectopic duct-like structures appear that express a variety of β-cell markers, including dense core granules visible by electron microscopy (EM). Use of a vector also expressing GFP shows that the ducts persist long after the viral gene expression has ceased, indicating that this is a true irreversible cell reprogramming event. We have recovered the insulin$^+$ cells by cell sorting and shown that they display glucose-sensitive insulin secretion. The early formed insulin$^+$ cells can be seen to coexpress SOX9 and are also labeled in mice lineage labeled for *Sox9* expression. SOX9$^+$ cells are normally found associated with small bile ducts in the periportal region, indicating that the duct-like structures arise from this source. This work confirms that developmentally related cells can be reprogrammed by suitable transcription factors and also suggests a unique therapy for diabetes.

It is now known that cell differentiation type can be reprogrammed by overexpression of selected transcription factors, usually a subset of those required for formation of the relevant cell type during normal development. Recent examples are the conversion of fibroblasts to cardiomyocytes, neurons, and hepatocytes (1–4). The formation of induced pluripotent stem cells may also be regarded as a type of cell type transformation (5–7). In 2008, Zhou et al. described a reprogramming of pancreatic exocrine cells to β-like cells, in vivo, by introduction of genes for the three transcription factors PDX1, NGN3, and MAFA (8). PDX1 controls growth and development of the pancreatic bud, NGN3 is required for formation of endocrine progenitors, and MAFA (and also PDX1 again) is required for maturation of β cells (9–11).

In this paper, we describe the effects of this gene combination on the liver. We were motivated to investigate this because the liver and pancreas are closely related in embryonic development, arising from adjacent regions of the endodermal epithelium of the foregut. In the early mouse embryo the distinction between the ventral pancreatic bud and the adjacent liver bud is caused by FGF and bone morphogenetic protein signaling from the adjacent mesenchyme (12–14). This relationship may mean that the chromatin configuration of mature liver cells still allows access to pancreatic transcription factors and so their overexpression can be effective at phenotypic reprogramming (15, 16). In addition to hepatocytes, the liver bud forms a system of bile ducts. These arise in the second half of gestation from structures called ductal plates, which form around the portal veins (17). The *Sox9* gene is expressed in early cells of the ductal plates and its expression persists in small but not large bile ducts after birth (18, 19).

We have studied events in the liver following delivery of *Pdx1*, *Ngn3*, and *MafA*. The genes were assembled into a single adenoviral vector, which was delivered i.v. to immunodeficient mice that had previously been made diabetic by administration of streptozotocin (STZ). Immunodeficient mice were used, as in the study of the pancreas (8), because immunocompetent mice gradually reject virus-transduced cells over a period of weeks (20). We see the formation of ectopic duct-like structures that express a range of typical β-cell markers, including dense core granules visible by electron microscopy (EM), exhibit glucose-stimulated insulin secretion, and develop from the SOX9$^+$ progenitors in the periportal region. The ectopic insulin$^+$ ducts are stable long term in the absence of viral DNA expression and so represent a real phenotypic reprogramming event. However, the ectopic ducts do not show a typical β-cell phenotype. They represent a stable, but unique cell type with sufficient β-cell properties to relieve diabetes.

Results

***Ad-PNM* Gives Long-Term Diabetes Relief with the Formation of Ectopic Insulin-Producing Ducts.** The adenoviral polycistronic constructs, *Ad-PNM* and *Ad-EGFP-PNM* (Fig. 1*A*), were constructed as described in *Materials and Methods*. When transduced into tissue culture cells, all three of the encoded proteins are produced at levels easily detected by immunostaining (Fig. S1 *A–C*). Western blots indicated that migration of the three proteins was consistent with the predicted molecular weight, indicating proper cleavage of the proteins by the 2A peptide upon translation (Fig. S1*D*). When injected into mice by tail vein injection, gene expression is essentially confined to the liver and is not seen in the pancreas or other parts of the gut (Fig. S2 *A* and *B*). Immunostaining for the vector-delivered gene products, PDX1, NGN3, and MAFA, showed their presence in many cells of the liver 1 wk after administration (Fig. S2 *C–E*).

NOD-SCID mice were injected with streptozotocin to induce diabetes. This drug destroys the β cells of the pancreas and its effects can be monitored by observing the elevation of blood glucose from 120 mg/dL to 360–500 mg/dL. Delivery of *Ad-PNM* or *Ad-EGFP-PNM* to diabetic NOD-SCID mice resulted in a rescue of the diabetes with a consistent maintenance of normal blood glucose levels over a period of at least 4 mo (Fig. 1*B*). About 80% of mice responded as shown. About 10% became hypoglycemic and died within 2 wk of the virus injection. A slight long-term decline of blood glucose is apparent but as it lies within the error bars we do not consider it to be significant. Although regeneration of β cells in mice treated with streptozotocin has been described (21), we found no regeneration in the pancreas of the treated mice during the time span of these experiments (Fig. S3), so we consider that the relief of diabetes

Author contributions: A.B., J.R.D. and J.M.W.S. designed research A.B., E.A., and J.R.D. performed research; E.A. and L.V.G. contributed new reagents/analytic tools; A.B., E.A., and J.M.W.S. analyzed data; and A.B. and J.M.W.S. wrote the paper.

The authors declare no conflict of interest.

This article is a PNAS Direct Submission. K.S.Z. is a guest editor invited by the Editorial Board.

Freely available online through the PNAS open access option.

[1]To whom correspondence should be addressed. E-mail: slack017@umn.edu.

This article contains supporting information online at www.pnas.org/lookup/suppl/doi:10.1073/pnas.1201701109/-/DCSupplemental.

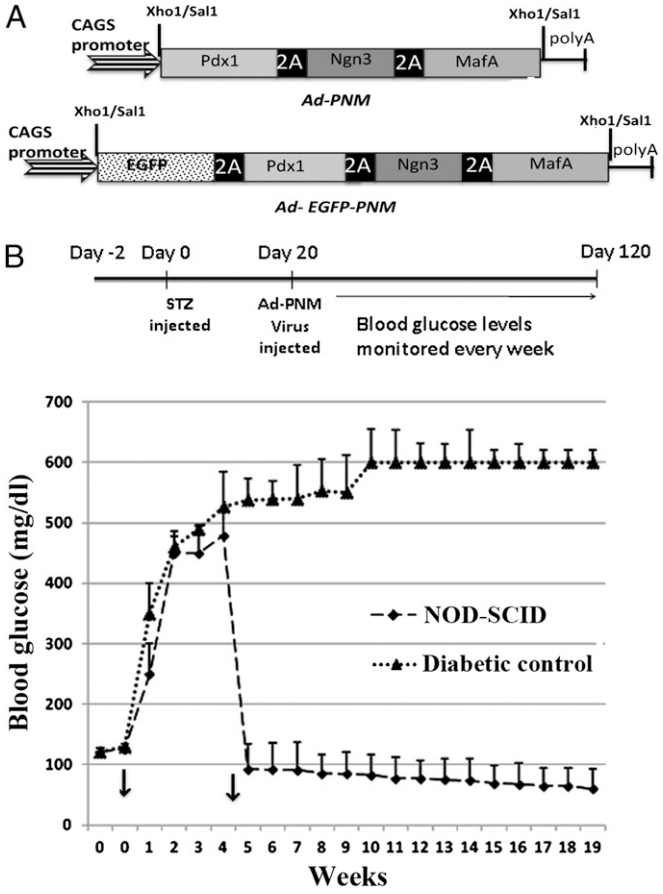

Fig. 1. Persistent normoglycemic levels are maintained following *Ad-PNM* delivery. (*A*) Diagrams of the vectors. (*B*) Long-term maintenance of normal blood glucose levels compared with diabetic controls (n = 5 per curve). Arrows show the time of STZ injection (week 0) and the time of *Ad-PNM* delivery (between weeks 4 and 5). The attenuation in blood glucose level is observed a few days after *Ad-PNM* delivery.

to be due to insulin synthesis by cells within the liver. The total insulin content in treated liver was 292 ± 30.6 pg/μg protein, compared with 12 ± 15.2 pg/μg protein in diabetic mice not given *Ad-PNM*.

In the livers of responding mice, we found discrete clusters of cells with a ductal morphology, but immunopositive for insulin (Fig. 2 *A*–*C*). The insulin immunofluorescence is cytoplasmic and granular in appearance (Fig. S4*A*). The insulin$^+$ cells are initially (1–2 wk from *Ad-PNM* administration) visible as small clusters. Later (3–16 wk from *Ad-PNM* administration) they become duct-like. These ectopic ducts are composed of uniform, low columnar, closely spaced epithelium, positive for CK19 and E-cadherin (Fig. 3). They are invested with small blood capillaries that could provide a route for insulin to enter the bloodstream (Fig. 2*C* and Fig. S4*D*). Transmission electron microscopy showed the presence of dense core granules in the cytoplasm of the duct cells, which are very similar to those seen in normal mouse β cells (Fig. 2 *E* and *F* and Fig. S4 *B* and *C*). Dense core granules are characteristic of insulin secretory granules, being electron dense because of the zinc, which is a component of the insulin crystals (22). The number of dense core granules is fewer than seen in normal β cells, and some nondense core granules of similar size are also seen, which may perhaps be secretory granules for other hormones (see below).

Liver damage in these experiments was assessed by monitoring of the serum for total bilirubin, alanine aminotransferase, and aspartate transaminase. There is a slight increase in total bilirubin following STZ treatment but no further statistically significant increase in any of the three measures following the *Ad-PNM* administration (Fig. S5). At no time did we see any tumor formation or other liver pathology.

When the *Ad-EGFP-PNM* vector was used, initially (weeks 1–4 postadministration) a very high proportion of cells in the liver become transduced and expressed GFP, as well as the three vector-encoded products: PDX1, NGN3, and MAFA. Accordingly the insulin$^+$ cell clusters visible at early stages are all GFP$^+$ (Fig. 2*A*). However, after 4 wk, the viral gene expression has largely decayed and only traces of GFP are left, often well separated from the insulin$^+$ structures (Fig. 2*B*). Moreover the NGN3 expression is no longer visible (Fig. S6*A*), whereas PDX1 and MAFA, which are expressed in normal β cells, persist (see below). This shows that the new phenotype persists in the absence of the initiating viral-encoded transcription factors.

Apart from insulin, the ducts displayed a number of other proteins characteristic of developing or mature β cells (Fig. 3). The structures are positive for C-peptide, indicative of synthesis of insulin rather than uptake and storage from the blood. PDX1

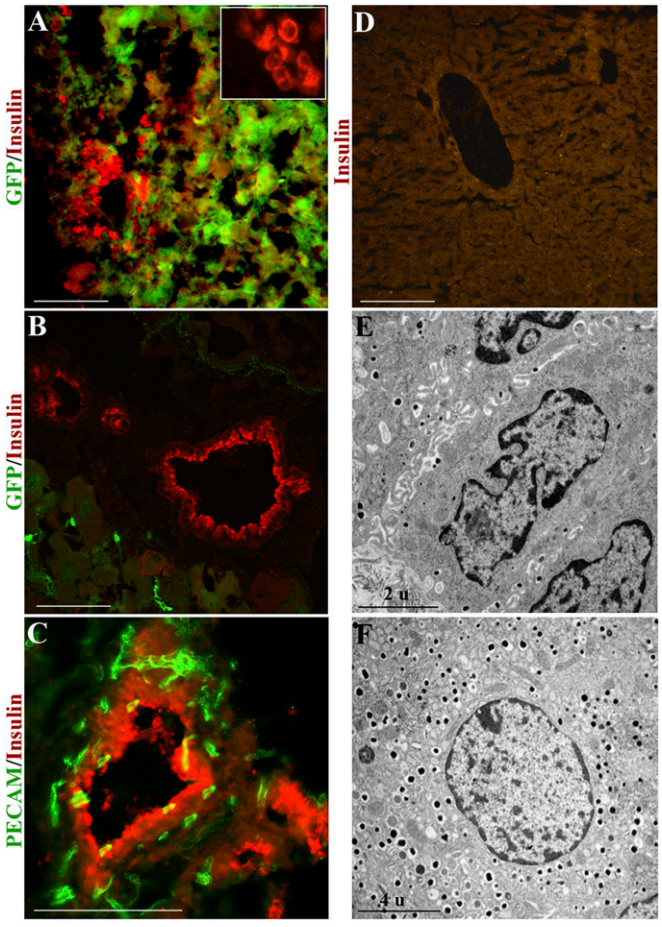

Fig. 2. Ectopic insulin$^+$ ducts in the liver. (*A*) Insulin$^+$ cells appear as small clusters and are mostly EGFP$^+$ 1 wk after *Ad-EGFP-PNM*. *Inset* shows the presence of insulin in the cytoplasm (red color only). (*B*) Absence of EGFP from the ductal structures after 4 wk. (*C*) Platelet endothelial cell adhesion molecule (PECAM) staining of the insulin$^+$ ducts shows the presence within the duct walls of small blood vessels. (*D*) Absence of insulin staining in control liver of diabetic mouse. (*E*) TEM shows the presence of dense core granules in the cytoplasm of duct cells. (*F*) Dense core granules in β cell of a normal mouse islet. In this and other figures, pictures represent at least three independent experiments. (Scale bars, 100 μm.)

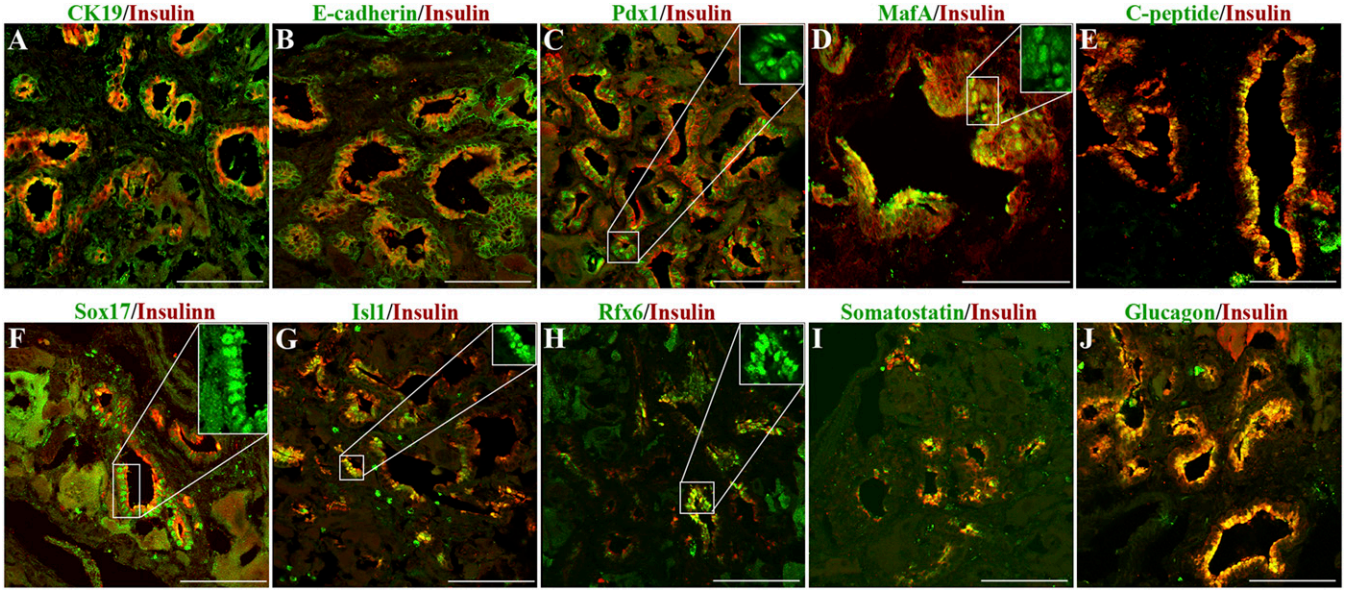

Fig. 3. Ectopic ducts express markers for β cells. (*A*) CK-19. (*B*) E-cadherin. (*C*) PDX1. (*D*) MAFA. (*E*) C-peptide. (*F*) SOX17. (*G*) ISL1. (*H*) RFX6. (*I*) Somatostatin. (*J*) Glucagon. (Scale bars, 100 μm.) Cases shown in *F* and *I* are from mice dosed with *Ad-EGFP-PNM*, so there are some patches of cytoplasmic GFP visible in addition to the antibody fluorescence. All cases are shown 12 wk after *Ad-PNM*. *Insets* show the nuclear localization of transcription factors.

was found to be present in all parts of the ducts, and we found MAFA, ISL1, RFX6, and SOX17 expressed in many cells. However, these structures also differ from mature β cells in several respects. They have the morphology of ducts and express CK19 and E-cadherin. They also express some other pancreatic endocrine hormones apart from insulin, including glucagon and somatostatin (Fig. 3).

Isolation of Insulin$^+$ Cells. Cells were isolated from the livers of killed mice by collagenase perfusion. Insulin is normally stored in β cells as crystals containing zinc, so the cells were stained with Newport Green, a fluorescent dye that binds selectively to zinc (23) (Fig. 4 *A*–*C*). Upon FACS analysis, 6–10% of the cells were selected as positive for Newport Green (Fig. S7*A*). To exclude artifacts due to uptake of Newport Green by dead cells, 7-AAD was added and the 7-AAD$^+$ cells were excluded from the sort. Liver from mice given *Ad-GFP* did not contain any Newport Green$^+$ cells (Fig. S7*B*).

qRT-PCR analysis of the isolated Newport Green$^+$ cells in comparison with the negative cells gave results consistent with the immunostaining of the intact livers (Fig. 4*D*). There is an increased expression of β-cell transcripts like *Insulin 1*, *Insulin 2*, *Pdx1*, *Isl1*, *MafA*, *NeuroD1*, *Rfx6*, and *Mnx1*. Interestingly the genes for components of the glucose-sensing mechanism, comprising glucose metabolizing (*Gck* and *Glut2*) and potassium channel (*Kcnj11* and *Abcc8*) proteins were found to be increased. Expression of *Slc30a8*, which encodes the zinc binding protein ZnT8, is high, consistent with both the Newport Green staining and the presence of the dense core granules in the EM. The Newport Green$^-$ cells were much higher in the hepatocyte markers

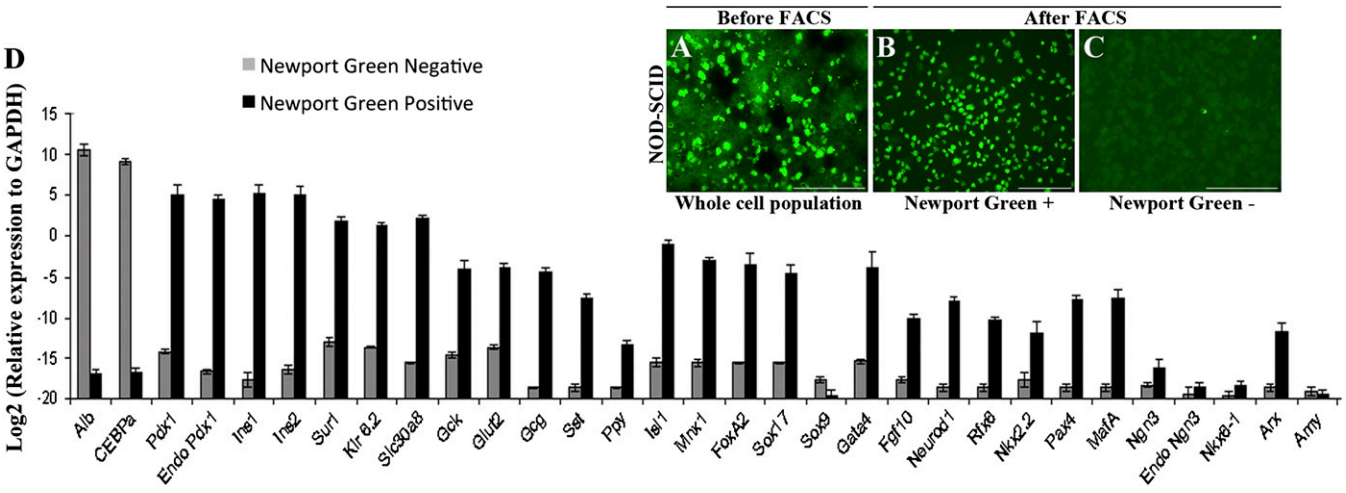

Fig. 4. Isolation of insulin$^+$ cells by Newport Green staining and FACS. Newport Green-stained cells before sorting (*A*) and after sorting (*B* and *C*). (*D*) qRT-PCR analysis of sorted cells. Ct values were normalized to *Gapdh* gene expression within the same cDNA sample. Results are presented as fold increase based on *Gapdh* gene expression and the values on the *y* axis represent log2 multiples of the *Gapdh* value, which is represented by 0. The data are means of three independent experiments on livers collected 12 wk after *Ad-PNM* administration. (Scale bars, 100 μm.)

Albumin and *C/ebpα*. *Amylase* expression was not noticed at any point, indicating the endocrine rather than exocrine nature of the reprogrammed ductal structures. The phenotype of the Newport Green$^+$ cells indicates a strong resemblance to the mature β-cell phenotype, although there are also differences from normal mouse islets (Fig. S7*C*). The insulin protein content of the Newport Green$^+$ cells was 1.29 ± 0.41 ng/μg total protein, whereas the content for normal mouse islets was 5.59 ± 1.42 ng/μg total protein. This insulin content of about 23% of normal islets is consistent with the results from electron microscopy (Fig. 2 *E* and *F*) and with the insulin secretion data (see below).

The presence of endogenous *Pdx1*, measured using primers to the 3′ UTR of the message, together with the very low levels of total *Ngn3* expression, is good evidence that the new phenotype is stable in the absence of vector gene expression, confirming the conclusion from the immunostaining presented above. The low endogenous *Ngn3* is similar to what would be expected in mature β cells.

Insulin$^+$ Ductal Cells Are Glucose Responsive. The fact that the diabetes induced by STZ was relieved does not prove that the insulin$^+$ cells are necessarily glucose responsive. To determine whether the mice were capable of glucose-sensitive insulin secretion, i.p. glucose tolerance tests were performed. The glucose challenge showed that the treated mice had glucose disposal much better than the diabetic controls, and approaching that of the nondiabetic controls. This was correlated with a glucose-stimulated elevation in serum insulin, indicating responsiveness of the insulin$^+$ cells to glucose (Fig. 5 *A* and *B*).

We also obtained a direct measure of glucose-sensitive insulin secretion. Newport Green$^+$ cells were isolated as above and were incubated in Krebs Ringer buffer for 2 h followed by addition of glucose at 2 or 20 mM. A fivefold increase in insulin release occurred following the glucose challenge. Although the magnitude of insulin secretion was only about 20% of control mouse islets, this shows that insulin secretion is glucose regulated and not constitutive, as is often the case for cells showing ectopic insulin production (Fig. 5 *C* and *D*). The lower level of insulin release than islets is consistent with the lower number of dense core granules observed in the EM study.

Origin of Insulin$^+$ Cells. During the first 2 wk following *Ad-PNM* administration, the insulin$^+$ cells are found also to be SOX9$^+$ (Fig. 6*A*). After about 4 wk, the SOX9 expression reduces (Fig. S6*B*). At no stage is there any presence of albumin in the ductal structures (Fig. 6*B*). This indicates that the insulin$^+$ ducts do not arise from hepatocytes and instead likely arise from a SOX9$^+$ population, for example those present in the small bile ducts or peribiliary glands.

We have confirmed this with the use of a *Sox9-CreER* mouse strain (19). It has been shown that *Sox9* is up-regulated in adult hepatocytes by tamoxifen, making it difficult to label *Sox9*$^+$ cells in adulthood (19). However, this problem does not exist in fetal animals and we were able to obtain mice with labeled biliary systems by administering tamoxifen in late pregnancy. A single dose of tamoxifen was injected into pregnant female mice from intercrosses between *Sox9-CreERT2* and *mT/mG* at embryonic day 15.5 (E15.5). Cells expressing *Sox9* should contain the CreER. On treatment with tamoxifen, all or most of them should excise the *tdTomato* gene from the reporter cassette, leading to expression of membrane bound GFP (mGFP). After birth, mGFP labeling was seen almost exclusively in the interlobular ductules and ducts, which continue to express SOX9 into adult life (Fig. 6 *C* and *D*). Mice were made diabetic with STZ, were given *Ad-PNM*, and showed an amelioration of diabetes. These mice are not immunodeficient, and so fewer insulin$^+$ ducts arise compared with NOD-SCIDs. However, some insulin$^+$ ducts are found, and these proved also to be positive for mGFP, confirming an origin from a *Sox9*$^+$ cell population (Fig. 6 *E* and *F*).

Discussion

Our results show that the three-gene combination *Pdx1*, *Ngn3*, and *MafA*, shown by Zhou et al. to reprogram pancreatic exocrine cells to a β-like state (8), is also capable of reprogramming cells in the liver to insulin$^+$ cells. These have some properties of pancreatic β cells but also display some novel characteristics.

The predominant insulin$^+$ cell type is the duct-like structure. These express typical markers such as E-cadherin and CK19, but they are also insulin$^+$ and C-peptide$^+$. Various β-cell transcription factors and glucose-sensing components are present, and the cells display glucose-sensitive insulin secretion, releasing about 20% as much insulin as normal mouse islets. However, these cells also produce significant levels of other pancreatic hormones (glucagon and somatostatin), and show a low level of *Nkx2.2* and *Nkx6.1*. Use of the *Ad-EGFP-PNM* vector shows that the ductal structures are initially GFP$^+$, but after some weeks the GFP, and also the NGN3 expression, is lost. This shows that the structures result from a genuine reprogramming event that is stable long term in the absence of the initiating factors.

The ectopic ducts do not correspond to any normal cell type found in the early pancreatic bud endoderm, or the transient population of multihormone cells in the developing pancreas, or the mature biliary or pancreatic ducts. In the normal extrahepatic biliary system (24, 25) and in certain pathologies involving β-cell neogenesis (26, 27), it is possible to find pancreatic endocrine cells budding off ducts, but in our case it is the actual cells of the ducts themselves that are producing the hormones. We have also shown that multihormone-producing cells can exhibit glucose-sensitive insulin secretion. For these various reasons we consider that the insulin$^+$ ducts represent a completely unique cell state.

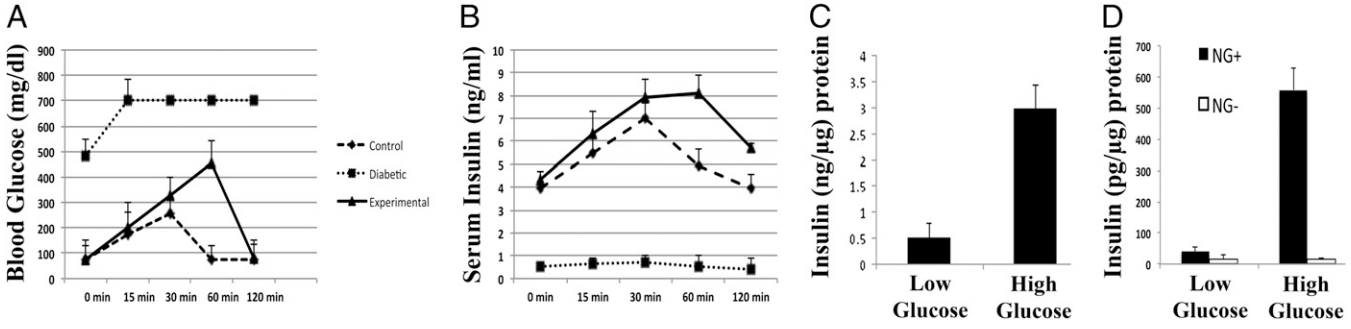

Fig. 5. Insulin$^+$ cells secrete insulin in response to glucose. (*A*) Plasma glucose. (*B*) Serum insulin levels following i.p. injection of glucose (n = 3). (*C*) Measurement of glucose-stimulated insulin release from mouse islets. (*D*) Measurement of glucose-stimulated insulin release from the Newport Green$^+$ and Newport Green$^-$ cells, sorted from liver of *Ad-PNM*–treated mice. Results are mean ± SE (n = 3).

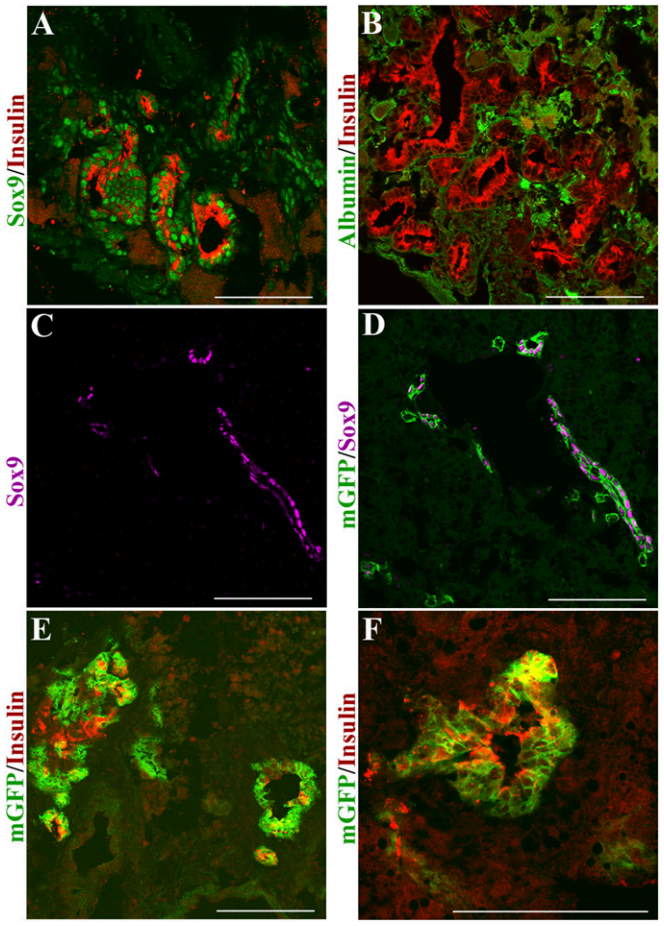

Fig. 6. Origin of ectopic ducts from SOX9$^+$ cells. (*A*) Insulin$^+$ ducts costain for SOX9. (*B*) They do not costain for albumin. Specimens 10 d after *Ad-PNM* administration. (*C* and *D*) Control *Sox9-CreERT2; mTmG* mouse labeled by tamoxifen treatment at E15.5 shows GFP in cells of the small bile ducts. SOX9 is shown in lilac, representing far red; GFP is green. (*E* and *F*) Insulin$^+$ structures induced by *Adeno-PNM* arise from GFP-labeled cells. Insulin is shown in red, representing far red. Two mice were analyzed. (Scale bars, 100 μm.)

We consider that the ducts do not derive from hepatocytes as there is no costaining with albumin at any stage. They do costain for SOX9 for the first 2 wk after *Ad-PNM* administration. Moreover the experiments with the *Sox9-CreER; mTmG* mice show that they arise from cells labeled for *Sox9* expression at the ductal plate stage of development. These are probably small bile ducts (22, 23) but the cells of origin might also be hepatoblast-like progenitor cells, thought to be in the periportal region associated with small bile ducts (26, 27) or perhaps they derive from the peribiliary glands, which are associated with larger bile ducts and are reported to contain cells expressing markers characteristic of embryonic endoderm (18, 19, 28–32).

Several previous studies have been made of the effects of β-cell transcription factors overexpressed in the liver. The first series was by Ferber (33, 34) using *Pdx1* alone. Subsequent experiments used *Pdx1* (35), *NeuroD*, and *betacellulin* (36) and *Pdx1VP16* with *NeuroD* (37). Insulin production and diabetes rescue was often reported, although in some studies there was clearly some liver damage. None of the previous studies have shown the appearance of the insulin$^+$ ductal structures that we describe. Our study also indicates that the *Pdx1*, *Ngn3*, and *MafA* combination is more reliable and effective than those used previously, especially when administered in a single vector. The dose required in immunodeficient mice is not excessive and does not provoke any significant liver damage (Fig. S5). The study of Yechoor et al. (38) used *Ngn3* and *β-cellulin*, delivered by adeno-associated virus (AAV). In their work, hepatocytes expressed insulin for a few weeks and then lost it, whereas insulin$^+$ cells with a longer lifetime were proposed to arise from oval cells in the periportal region. We do also see some scattered insulin$^+$ cells resembling hepatocytes during the first few weeks. The periportal oval cells may very well be the same SOX9$^+$ cells that we believe are the progenitors. However, Yechoor et al. (38) did not observe ectopic insulin-producing ducts. Compared with their study, we find about a 10-fold higher level of insulin protein in the liver, indicating the greater effectiveness of the three-gene mixture. We were also able to prove, through the use of *Ad-EGFP-PNM*, that the insulin$^+$ ducts persist long after the cessation of viral gene expression and so the effect is one of genuine and permanent reprogramming.

This area of work has an obvious interest in terms of possible novel therapies for diabetes. Our study provides unique evidence for in vivo reprogramming of cells in the biliary tract to a β-cell–like phenotype, which is capable of relieving diabetes in adult individuals. The potential of gene delivery to the liver has been considered before (39–41) but we believe that the three-gene mixture used here is greatly superior to the previous methods in terms of dose and absence of liver damage. Moreover a single treatment is effective, and the effect does not require viral gene integration or persistent viral gene expression.

Materials and Methods

Construction of a Polycistronic Viral Vector Containing Three β-Cell Transcription Factors. Construction of the polycistronic construct *Ad-PNM* was described in ref. 42. Properties of the 2A sequence are described in ref. 43. Construction of the *Ad-EGFP-PNM* version was done by ligating a *EGFP-2A* fragment in front of the *Pdx1* gene as a Sal/Xho fragment.

Induction of Diabetes and Delivery of Transcription Factors. All animal experiments were approved by the institutional animal care and use committee of the University of Minnesota. Diabetes was induced in mice with an i.p. injection of streptozotocin (STZ) (Sigma) at a dose of 120 mg/kg body weight. Blood glucose was measured with an Accu-Chek glucose meter (Roche). Mice showing a blood glucose levels in the range of 360 to 600 mg/dL over at least 7 d were considered as diabetic and were used for treatment with *Ad-PNM* or *Ad-EGFP-PNM*. The standard dose used for the NOD-SCID mice was 150 μL of 10^{10} pfu/mL (i.e., 1.5×10^9 pfu per mouse), injected into the tail vein.

Immunohistochemistry. Livers were either fixed in 4% (wt/vol) paraformaldehyde made in PBS, pH 7.4, or in 10% (vol/vol) formalin buffered with PBS (Fischer) for 2 h or overnight at room temperature and were either frozen in optimal cutting temperature compound (OCT) or embedded in paraffin. Sections of 5–7 μm were cut and paraffin-embedded sections were subject to antigen retrieval with sodium citrate, pH 6 for 20 min using a vegetable steamer. Sections were permeabilized with 1% Triton X-100 for 20 min, blocked in 10% (vol/vol) goat or sheep serum, and incubated with the appropriate primary antibody overnight at 4 °C. Then they were washed in PBS and incubated with Alexa Fluor conjugated secondary antibody for 1 h to visualize the required immunofluorescence staining.

The list of primary antibodies is given in Table S1.

Electron Microscopy. Livers of *Ad-PNM*-treated mice were fixed in 2.5% (vol/vol) glutaraldehyde and 0.1 M sodium cacodylate, pH 7.4 for 2 h at room temperature and then overnight at 4 °C. For transmission electron microscopy (TEM), samples were further fixed with 1% osmium tetroxide/0.1 M sodium cacodylate buffer, dehydrated, embedded in Epon resin, and sectioned at 1 μm. Ectopic ductal structures were localized with Toluidine Blue staining and ultrathin sections of 60 nm were cut from the same region on a Leica U6 Ultracut-S microtome, picked up onto copper grids, stained with 0.2% lead citrate for 5 min, and examined in a JEOL 1200EX transmission electron microscope.

ELISA. Insulin was extracted from the liver tissues of the responding mice by an acid-ethanol (1:37) method containing (1:10) protease inhibitor mixture (Sigma). The cells were lysed and left on a rotator overnight at 4 °C. The

mixture was centrifuged at 15,700 × *g* for 10 min to separate supernatant and pellet, and the pellet was dissolved in 100 mM NaOH. The total protein in supernatant and dissolved pellet was measured using the Protein Measurement kit (Pierce). The insulin levels in the supernatant and dissolved pellet were measured using an Ultrasensitive ELISA kit for mouse (Alpco) according to the manufacturer's instructions.

Newport Green Staining, Cell Sorting, and Glucose Sensitivity. Labeling with Newport Green diacetate, (NG-Ac; Invitrogen) was done on isolated liver cells from mice that had responded to *Ad-PMN*. Cells were washed twice with PBS and then incubated for 30 min at 37 °C with PBS containing 1–10 μM NG-Ac plus 1 μL/mL Pluronic F127 (Sigma) to aid penetration of the dye. After washing in PBS with 5% (vol/vol) FCS, the cells were resuspended and the single-cell suspension was subjected to fluorescence microscopy and FACS analysis.

Quantitative Reverse Transcription PCR (qRT-PCR). RNA isolation and cDNA synthesis from the Newport Green$^+$ and Newport Green$^-$ cells were performed by using a Qiagen RNeasy micro Isolation kit, SuperScript II, and Oligo-dT or random primers (Invitrogen) according to the manufacturer's instructions. Primers used for qRT-PCR are listed in Table S2.

Labeling of SOX9$^+$ Cells. *Sox9-CreERT2; mT/mG* double heterozygous animals were generated by mating homozygous *Sox9CreERT2* males with *mT/mG*, a double-fluorescent Cre reporter mouse that expresses membrane-targeted tandem dimer (td)Tomato (mT) before Cre-mediated excision and membrane-targeted green fluorescent protein (mG) after excision (44). Tamoxifen (Sigma) was dissolved in sunflower seed oil at a concentration of 10 mg/mL and injected intraperitoneally to pregnant mice at a dose of 3 mg. The stage of pregnancy was day 15 (E15.5) to label the *Sox9*$^+$ cells of the ductal plates. Five-week-old postnatal *Sox9CreERT2; mT/mG* mice were made diabetic with streptozotocin at a dose of 120 mg/mL. Mice having a blood glucose level above 400 mg/dL were injected with *Ad-PNM* and cryosections were prepared of the livers. These were analyzed for GFP fluorescence and for SOX9 and insulin by immunostaining. Because the mice also contain the tdTomato label, far red conjugates were used for the secondary antibodies.

ACKNOWLEDGMENTS. We thank Genya Gekker for assistance with cell sorting; Doug Melton (Harvard University) for the three single adenovectors encoding PDX1, NGN3, and MAFA; Maike Sander (University of California, Irvine) for the *Sox9-CreER2* mice; and Cliff Steer and Yasu Kawakami for useful advice. This work was supported by National Institutes of Health Grant R01DK080747 and University of Minnesota Grant TRG 08-12.

1. Ieda M, et al. (2010) Direct reprogramming of fibroblasts into functional cardiomyocytes by defined factors. *Cell* 142:375–386.
2. Vierbuchen T, et al. (2010) Direct conversion of fibroblasts to functional neurons by defined factors. *Nature* 463:1035–1041.
3. Huang P, et al. (2011) Induction of functional hepatocyte-like cells from mouse fibroblasts by defined factors. *Nature* 475:386–389.
4. Sekiya S, Suzuki A (2011) Direct conversion of mouse fibroblasts to hepatocyte-like cells by defined factors. *Nature* 475:390–393.
5. Takahashi K, Yamanaka S (2006) Induction of pluripotent stem cells from mouse embryonic and adult fibroblast cultures by defined factors. *Cell* 126:663–676.
6. Meissner A, Wernig M, Jaenisch R (2007) Direct reprogramming of genetically unmodified fibroblasts into pluripotent stem cells. *Nat Biotechnol* 25:1177–1181.
7. Okita K, Ichisaka T, Yamanaka S (2007) Generation of germline-competent induced pluripotent stem cells. *Nature* 448:313–317.
8. Zhou Q, Brown J, Kanarek A, Rajagopal J, Melton DA (2008) In vivo reprogramming of adult pancreatic exocrine cells to beta-cells. *Nature* 455:627–632.
9. Murtaugh LC, Melton DA (2003) Genes, signals, and lineages in pancreas development. *Annu Rev Cell Dev Biol* 19:71–89.
10. Gittes GK (2009) Developmental biology of the pancreas: A comprehensive review. *Dev Biol* 326:4–35.
11. McKnight KD, Wang P, Kim SK (2010) Deconstructing pancreas development to reconstruct human islets from pluripotent stem cells. *Cell Stem Cell* 6:300–308.
12. Deutsch G, Jung J, Zheng M, Lóra J, Zaret KS (2001) A bipotential precursor population for pancreas and liver within the embryonic endoderm. *Development* 128: 871–881.
13. Zaret KS (2008) Genetic programming of liver and pancreas progenitors: Lessons for stem-cell differentiation. *Nat Rev Genet* 9:329–340.
14. Zaret KS, Grompe M (2008) Generation and regeneration of cells of the liver and pancreas. *Science* 322:1490–1494.
15. Slack JMW (1985) Homoeotic transformations in man: Implications for the mechanism of embryonic development and for the organization of epithelia. *J Theor Biol* 114: 463–490.
16. Slack JMW (2007) Metaplasia and transdifferentiation: From pure biology to the clinic. *Nat Rev Mol Cell Biol* 8:369–378.
17. Shiojiri N (1997) Development and differentiation of bile ducts in the mammalian liver. *Microsc Res Tech* 39:328–335.
18. Antoniou A, et al. (2009) Intrahepatic bile ducts develop according to a new mode of tubulogenesis regulated by the transcription factor SOX9. *Gastroenterology* 136: 2325–2333.
19. Carpentier R, et al. (2011) Embryonic ductal plate cells give rise to cholangiocytes, periportal hepatocytes, and adult liver progenitor cells. *Gastroenterology* 141: 1432–1438.
20. Yang Y, et al. (1994) Cellular immunity to viral antigens limits E1-deleted adenoviruses for gene therapy. *Proc Natl Acad Sci USA* 91:4407–4411.
21. Grossman EJ, et al. (2010) Glycemic control promotes pancreatic beta-cell regeneration in streptozotocin-induced diabetic mice. *PLoS ONE* 5:e8749.
22. Lemaire K, et al. (2009) Insulin crystallization depends on zinc transporter ZnT8 expression, but is not required for normal glucose homeostasis in mice. *Proc Natl Acad Sci USA* 106:14872–14877.
23. Lukowiak B, et al. (2001) Identification and purification of functional human beta-cells by a new specific zinc-fluorescent probe. *J Histochem Cytochem* 49:519–528.
24. Dutton JR, et al. (2007) Beta cells occur naturally in extrahepatic bile ducts of mice. *J Cell Sci* 120:239–245.
25. Eberhard D, Tosh D, Slack JMW (2008) Origin of pancreatic endocrine cells from biliary duct epithelium. *Cell Mol Life Sci* 65:3467–3480.
26. Gu D, Sarvetnick N (1993) Epithelial cell proliferation and islet neogenesis in IFN-g transgenic mice. *Development* 118:33–46.
27. Lipsett M, Finegood DT (2002) β-cell neogenesis during prolonged hyperglycemia in rats. *Diabetes* 51:1834–1841.
28. Dorrell C, et al. (2011) Prospective isolation of a bipotential clonogenic liver progenitor cell in adult mice. *Genes Dev* 25:1193–1203.
29. Shin S, et al. (2011) Foxl1-Cre-marked adult hepatic progenitors have clonogenic and bilineage differentiation potential. *Genes Dev* 25:1185–1192.
30. Nakanuma Y, Hoso M, Sanzen T, Sasaki M (1997) Microstructure and development of the normal and pathologic biliary tract in humans, including blood supply. *Microsc Res Tech* 38:552–570.
31. Carpino G, et al. (2012) Biliary tree stem/progenitor cells in glands of extrahepatic and intraheptic bile ducts: An anatomical in situ study yielding evidence of maturational lineages. *J Anat* 220:186–199.
32. Furuyama K, et al. (2011) Continuous cell supply from a Sox9-expressing progenitor zone in adult liver, exocrine pancreas and intestine. *Nat Genet* 43:34–41.
33. Ferber S, et al. (2000) Pancreatic and duodenal homeobox gene 1 induces expression of insulin genes in liver and ameliorates streptozotocin-induced hyperglycemia. *Nat Med* 6:568–572.
34. Ber I, et al. (2003) Functional, persistent, and extended liver to pancreas transdifferentiation. *J Biol Chem* 278:31950–31957.
35. Miyatsuka T, et al. (2003) Ectopically expressed PDX-1 in liver initiates endocrine and exocrine pancreas differentiation but causes dysmorphogenesis. *Biochem Biophys Res Commun* 310:1017–1025.
36. Kojima H, et al. (2003) NeuroD-betacellulin gene therapy induces islet neogenesis in the liver and reverses diabetes in mice. *Nat Med* 9:596–603.
37. Kaneto H, et al. (2005) PDX-1/VP16 fusion protein, together with NeuroD or Ngn3, markedly induces insulin gene transcription and ameliorates glucose tolerance. *Diabetes* 54:1009–1022.
38. Yechoor V, et al. (2009) Neurogenin3 is sufficient for transdetermination of hepatic progenitor cells into neo-islets in vivo but not transdifferentiation of hepatocytes. *Dev Cell* 16:358–373.
39. Efrat S (2002) Cell replacement therapy for type 1 diabetes. *Trends Mol Med* 8: 334–339.
40. Meivar-Levy I, Ferber S (2003) New organs from our own tissues: Liver-to-pancreas transdifferentiation. *Trends Endocrinol Metab* 14:460–466.
41. Sapir T, et al. (2005) Cell-replacement therapy for diabetes: Generating functional insulin-producing tissue from adult human liver cells. *Proc Natl Acad Sci USA* 102: 7964–7969.
42. Akinci E, Banga A, Greder LV, Dutton JR, Slack JMW (2012) Reprogramming of pancreatic exocrine cells towards a beta (β) cell character using Pdx1, Ngn3 and MafA. *Biochem J* 442:539–550.
43. de Felipe P (2004) Skipping the co-expression problem: The new 2A "CHYSEL" technology. *Genet Vaccines Ther* 2:13.
44. Muzumdar MD, Tasic B, Miyamichi K, Li L, Luo LQ (2007) A global double-fluorescent Cre reporter mouse. *Genesis* 45:593–605.